Organic Carbon Stocks and Accumulation Rates in Surface Sediments of the Norwegian Continental Margin

Markus Diesing[1], Sarah Paradis[2], Henning Jensen[1], Terje Thorsnes[1], Lilja R Bjarnadóttir[1], and Jochen Knies[1]

[1]Geological Survey of Norway
[2]Geological Institute, ETH Zürich

November 22, 2023

Abstract

The role that continental margin sediments play in the global carbon cycle and the mitigation of climate change is currently not well understood. Recent research has indicated that these sediments might store large amounts of organic carbon; however, Blue Carbon research continues to focus on vegetated coastal ecosystems as actionable Blue Carbon. Marine sediments are considered emerging Blue Carbon ecosystems, but to decide whether they are actionable requires better quantifications of organic carbon stocks, accumulation rates, and the mitigation potential from avoided emissions. To close some of these knowledge gaps, we spatially predicted organic carbon content, dry bulk density and sediment accumulation rates across the Norwegian margin. The resulting predictions were used to estimate organic carbon stocks in surface sediments and their accumulation rates. We found that organic carbon stocks are two orders of magnitude higher than those of vegetated coastal ecosystems and comparable to terrestrial ecosystems in Norway. Accumulation rates of organic carbon are spatially highly variable and linked to geomorphology and associated sedimentary processes. We identify shelf valleys with a glacial origin as hotspots of organic carbon accumulation with a potentially global role due to their widespread occurrence on formerly glaciated continental margins. The complex and heterogenous nature of continental margins regarding organic carbon accumulation means that to close existing knowledge gaps requires detailed spatial predictions that account for those complexities. Only in this way will it be possible to evaluate whether margin sediments might be actionable Blue Carbon ecosystems.

Organic Carbon Stocks and Accumulation Rates in Surface Sediments of the Norwegian Continental Margin

Markus Diesing[1], Sarah Paradis[2], Henning Jensen[1], Terje Thorsnes[1], Lilja Rún Bjarnadóttir[1], Jochen Knies[1,3]

[1] Geological Survey of Norway, P.O. Box 6315, Torgarden, 7491 Trondheim, Norway

[2] Department of Earth Sciences, Geological Institute, ETH Zürich, Sonneggstrasse 5, 8092 Zürich, Switzerland

[3] iC3: Centre for ice, Cryosphere, Carbon and Climate, Department of Geosciences, UiT The Arctic University of Norway, 9037 Tromsø, Norway

Corresponding author: Markus Diesing (markus.diesing@ngu.no)

Key Points:

- Continental margin sediments are an overlooked store of organic carbon in the context of Blue Carbon.
- Glacial troughs may be global hot spots of organic carbon accumulation.
- The role of continental margins in the carbon cycle is more complex than previously thought.

Abstract

The role that continental margin sediments play in the global carbon cycle and the mitigation of climate change is currently not well understood. Recent research has indicated that these sediments might store large amounts of organic carbon; however, Blue Carbon research continues to focus on vegetated coastal ecosystems as actionable Blue Carbon. Marine sediments are considered emerging Blue Carbon ecosystems, but to decide whether they are actionable requires better quantifications of organic carbon stocks, accumulation rates, and the mitigation potential from avoided emissions. To close some of these knowledge gaps, we spatially predicted organic carbon content, dry bulk density and sediment accumulation rates across the Norwegian margin. The resulting predictions were used to estimate organic carbon stocks in surface sediments and their accumulation rates. We found that organic carbon stocks are two orders of magnitude higher than those of vegetated coastal ecosystems and comparable to terrestrial ecosystems in Norway. Accumulation rates of organic carbon are spatially highly variable and linked to geomorphology and associated sedimentary processes. We identify shelf valleys with a glacial origin as hotspots of organic carbon accumulation with a potentially global role due to their widespread occurrence on formerly glaciated continental margins. The complex and heterogenous nature of continental margins regarding organic carbon accumulation means that to close existing knowledge gaps requires detailed spatial predictions that account for those complexities. Only in this way will it be possible to evaluate whether margin sediments might be actionable Blue Carbon ecosystems.

Plain Language Summary

To keep global average temperature rise well below 2°C requires drastic emission reductions and a removal of carbon dioxide from the atmosphere. Part of the carbon dioxide removal could be achieved by nature itself, if ecosystems that remove substantial amounts of carbon from the atmosphere are protected, managed, or restored. In the marine environment, the focus has been placed on coastal ecosystems with rooted vegetation, as they remove carbon at high rates, are threatened by human activities and are amenable to management. Collectively, these are called actionable Blue Carbon ecosystems. More recently, marine sediments have been put forward, but these are currently labelled emerging Blue Carbon ecosystems due to existing knowledge gaps. To close some of these gaps we mapped the amount of organic carbon stored in sediments of the Norwegian seafloor and the rates at which it is accumulated. We found that there is 100 times more organic carbon in the seabed than in vegetated coastal ecosystems in Norway. Rates of organic carbon accumulation vary in space and are highest in glacial troughs. To improve our estimates of how much carbon accumulates in marine sediments globally will require to consider the complex nature of the continental margins.

1 Introduction

The burial of organic carbon in seafloor sediments is crucial for moving carbon from the short-term surface to the long-term geological cycle (Keil, 2017). This long-term carbon cycle is, in turn, controlling the concentration of atmospheric carbon dioxide (CO_2) over geological timescales (Berner, 2003). The size of the organic carbon seafloor sink, and the relative contributions of the continental margins versus the deep-sea, have been a matter of research for the last 50 years or so. A first estimate, based on multiplying average organic carbon content of Holocene sediments by area and thickness, yielded 223 Tg C yr^{-1}, of which 10% and 88% are deposited on the continental shelf and slope, respectively (Gershanovich et al., 1974; cited in Hedges & Keil, 1995). Berner (1982) argued that organic carbon is preferentially buried in deltaic shelf sediments (83% of a total burial rate of 126 Tg C yr^{-1}). His estimates were subsequently revised by Hedges & Keil (1995) to account for organic carbon burial in sediments of the continental shelves and upper slopes, respectively, and estimated that roughly 90 % of organic carbon is buried in coastal and continental margin settings.

Routine collection of ocean colour data with satellites has made it possible to estimate primary production, particle export, bottom flux, and burial of organic carbon with spatial detail. Muller-Karger et al. (2005) estimated that continental margins may be responsible for >40% of the organic carbon sequestration in the ocean. An even higher estimate of 98% for margins was published by Dunne et al. (2007). The same authors also estimated that 85% of the total burial flux (0.67 ± 0.45 Pg C yr^{-1}) occurred on continental shelves (shallower than 200 m). The latter, however, is in contradiction to de Haas et al. (2002) suggesting that shelf areas do not accumulate substantial amounts of organic carbon under present day conditions and, only locally, are considerable amounts of organic carbon buried. De Haas et al. (2002) concluded that the role of shelves as sinks for organic carbon is overestimated due to recurrent hydrodynamic processes that prevent its deposition in comparison to deeper continental slopes.

More recently, it has been claimed that the importance of seafloor sediments as places of organic carbon sequestration is somewhat diminished in comparison to vegetated coastal ecosystems (saltmarshes, mangroves, and seagrass meadows), which would account for 46% of the marine organic carbon burial despite covering only 0.2% of the ocean surface (Duarte et al., 2005, 2013). Vegetated coastal ecosystems have been a focus of research over the last ten to fifteen years under the concept of Blue Carbon (Nellemann et al., 2009). As these ecosystems might be able to remove CO_2 from the atmosphere at high rates, store fixed CO_2 as organic carbon over timescales of centuries or longer, and are frequently threatened by human activities, it has been suggested that management, conservation, and restoration of vegetated coastal ecosystems might significantly contribute to greenhouse gas removal from the atmosphere (Lovelock & Duarte, 2019).

Other ecosystems might satisfy the above definition of actionable Blue Carbon, but research gaps currently preclude from a classification as such. Emerging Blue Carbon ecosystems include wild and cultivated macroalgae, unvegetated tidal flats, and marine sediments (Howard et al., 2023). Continental shelf and slope (margin) sediments might exhibit lower organic carbon stocks and accumulation rates per unit area but cover much larger areas than vegetated coastal ecosystems. The large spatial extent might weigh out the low areal stocks and accumulation rates, but the importance of continental margins as places of organic carbon accumulation and storage relative to vegetated coastal ecosystems is currently not well understood. While our knowledge on local, regional, and global organic carbon stocks has steeply increased over the past few years (Atwood et al., 2020; Diesing et al., 2017, 2021; Hunt et al., 2020; Lee et al., 2019; Legge et al., 2020; Smeaton et al., 2021; Wilson et al., 2018), there currently exist knowledge gaps regarding organic carbon accumulation in margin sediments. Specifically, we lack spatially explicit quantifications of organic carbon accumulation rates and related uncertainties in the estimates. Such knowledge gaps could be filled with the application of machine learning spatial models, as exemplified by Diesing et al. (2021). Accounting for the complex nature of continental margins with zones of rapid carbon cycling and accumulation juxtaposed (Diesing et al., 2021; de Haas et al., 2002) will be an important consideration.

This study investigates the significance of continental margin sediments in terms of organic carbon accumulation and storage potential. We do not aim to estimate organic carbon burial, as the reference depths below which organic carbon is assumed to be removed from the short-term surface carbon cycle vary between studies and organic carbon might not even be irreversibly buried or preserved (Bradley et al., 2022). Instead, we estimate the amount of organic carbon that accumulates in the seabed on a timescale of approximately 100 - 150 years. Specifically, we aim to answer how much organic carbon is accumulated and stored in surface sediments (0 – 10 cm) on the Norwegian continental margin and discuss its hotspot potential for carbon storage in contrast to vegetated coastal ecosystems and terrestrial ecosystems.

1.1 Study site

Our area of interest (Figure 1) comprises the Norwegian continental shelf and slope (after Harris et al., 2014), which we define here as the Norwegian continental margin. We also include shallow parts of the abyss (deep sea) within 50 km distance from the seaward boundary of the slope to make best use of existing data. We further subdivide the continental shelf into shallow shelf (above 200 m water depth), deep shelf (between 200 m water depth and the shelf break) and shelf valleys (irrespective of water depth), as mapped by Harris et al. (2014). On the formerly glaciated continental margin of Norway, most shelf valleys are of glacial origin and as such could also be considered as glacial troughs. Our study site spans 26° of latitude and approximately 3000 km between the North Sea and the Arctic Ocean north off Svalbard.

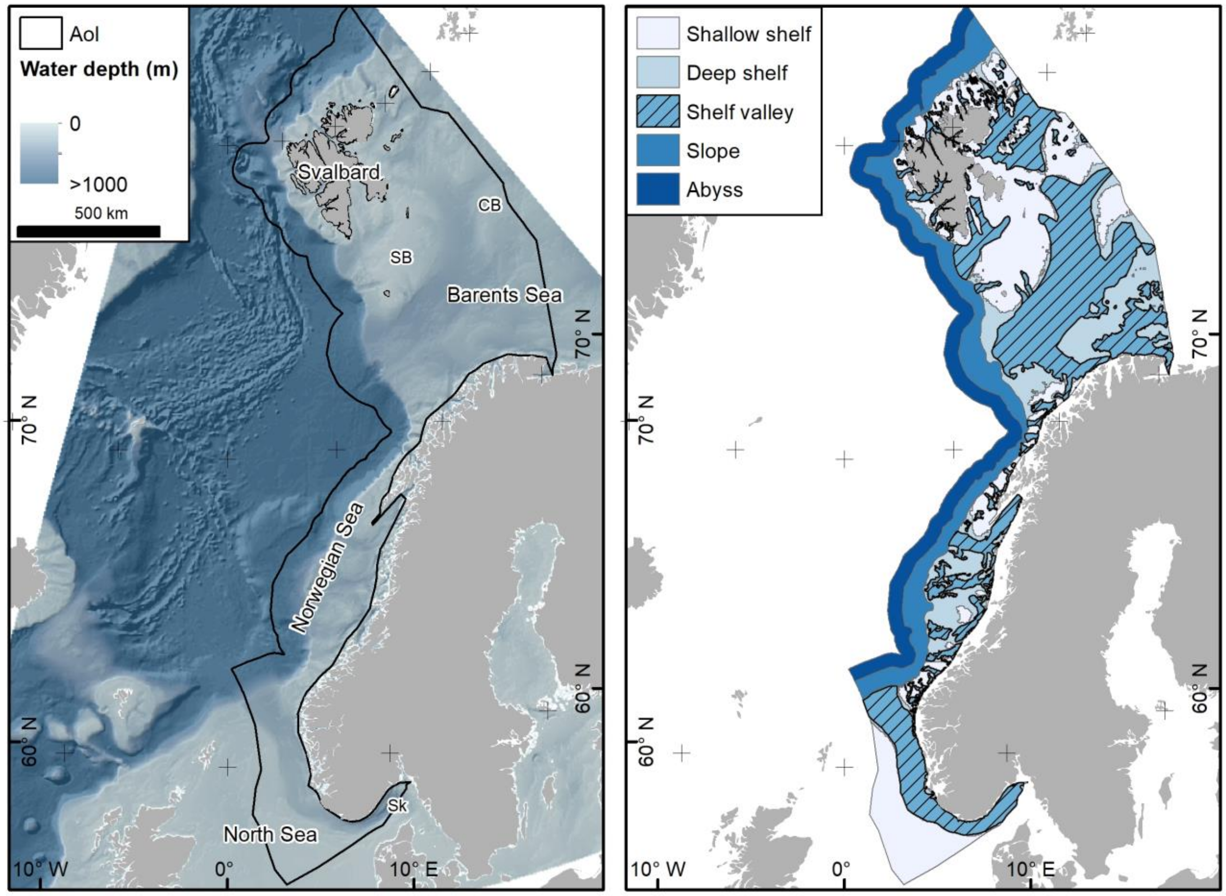

Figure 1. Overview of the area of interest (AoI): Left – Water depth (GEBCO Bathymetric Compilation Group, 2019), regional seas and locations mentioned in the text. CB – Central Bank, SB – Spitsbergen Bank, Sk – Skagerrak. Right – Geomorphological units based on Harris et al. (2014). The continental shelf is further subdivided into shallow shelf (0 to 200 m water depth) and deep shelf (200 m depth to the shelf edge).

2 Data

2.1 Response variables

To derive organic carbon stocks and accumulation rates it is necessary to spatially predict dry bulk density, organic carbon content, and sediment accumulation rates (also referred to as linear sedimentation rates). Several studies have shown that an important predictor for organic carbon content is the silt-clay (mud) content in seafloor sediments (Diesing et al., 2017; Wilson et al., 2018). As this important predictor layer did not exist in the area of interest, we spatially predicted it. We also predicted the spatial distribution of substrate types and the depositional environments and used the class probabilities as predictors. Substrate type is potentially an important predictor for mud content, dry bulk density, and organic carbon content, while the depositional environment might be important to predict sedimentation rates. Table 1 summarises the variables that have been estimated, how they were derived, and how they were used in the process we describe.

Table 1. Overview of variables that were estimated, how they were derived and how they were used. Reference is also made to the respective figures and repositories.

Variable	Derived by	Used	Figure	Repository
Substrate type	Spatial prediction	As predictor variable	S1	Zenodo
Depositional environment	Spatial prediction	As predictor variable	S2	Zenodo
Mud content	Spatial prediction	As predictor variable	S3	Zenodo
Dry bulk density	Spatial prediction	To calculate organic carbon stocks and accumulation rates	S4	Zenodo
Organic carbon content	Spatial prediction	To calculate organic carbon stocks and accumulation rates	S5	Zenodo
Sediment accumulation rate	Spatial prediction	To calculate organic carbon accumulation rates	S6	Zenodo
Organic carbon stock	Calculation (eq. 2)	For analysis	2	Pangaea
Organic carbon accumulation rate	Calculation (eq. 4)	For analysis	4	Pangaea

2.1.1 Substrate type and depositional environment

Maps of substrate type and depositional environment are routinely produced by expert interpretation at local, regional and overview scales as part of the Mareano seafloor mapping programme (www.mareano.no/en). However, these maps currently cover only a fraction of the Norwegian margin (Figures S1 and S2). We therefore decided to fill the existing coverage gaps by spatial prediction. We treated the existing maps as response data by converting the polygon shapefiles into raster data with a resolution of 4 km aligned to the predictor raster stack (see chapter 2.2 for details) using the Polygon to Raster function in ArcGIS 10.8.2, with maximum combined area as cell assignment type. The raster datasets were subsequently converted into point data (Raster to Point function) with the substrate type or depositional environment class as attribute. The original classifications contained more than 30 substrate types and six classes of depositional environment. These were simplified to eight substrate types and three classes of depositional environment, respectively (Table S1 and S2).

2.1.2 Mud content

Grain-size data (mud, sand, and gravel content) were obtained from the PANGAEA database (Felden et al., 2023), the ICES Data Portal contaminants dataset (https://data.ices.dk/), the Environmental Monitoring database MOD (DNV, 2023), the Geological Survey of Norway and the Mareano chemistry database (https://mareano.no/en/maps-and-data/chemical-data). Data were pre-processed by replacing records of 0 weight-% with 0.001 weight-% and rescaling to achieve fraction sums of 100 weight-% (Martín-Fernandéz & Thió-Henestrosa, 2006). This was necessary as additive log-ratios (Pawlowsky-Glahn & Olea, 2004) were subsequently calculated due to the compositional nature of the grain-size data.

2.1.3 Dry bulk density

Dry bulk density data were obtained from the PANGAEA database via a data warehouse query. The downloaded data were restricted to the upper 0.5 m of the sediment column. Furthermore, we used data on mud content from the Mareano chemistry database to calculate porosity (ϕ) according to an empirical equation (Jenkins, 2005) and ultimately dry bulk density (ρ_d) according to $\rho_d = (1 - \phi)\rho_s$ with grain density, ρ_s = 2.65 g cm^{-3}.

2.1.4 Organic carbon content and sediment accumulation rates

Data on organic carbon content and ^{210}Pb-derived sediment accumulation rates were obtained from the MOSAIC database (Paradis et al., 2023; van der Voort et al., 2020). The datasets included data from the Mareano chemistry database among others.

2.1.5 Pseudo samples

Datasets compiled from the literature or obtained from databases are frequently biased. For example, sediment accumulation rates are usually only reported in areas where sediments are deposited and caution is advised when spatially predicting such data (Jenkins, 2018). One strategy to deal with this limitation is to include pseudo-observations (Hengl et al., 2017); in this case records of 0 cm yr^{-1} sediment accumulation in areas that are erosional in nature. Similar approaches have previously been adopted by Diesing et al. (2021) and Mitchell et al. (2021). We randomly placed pseudo samples within the area predicted as Erosion or Transport (Figure S2). Additionally, we observed that coarse-grained sediments (muddy sandy gravel, sandy gravel, and gravel) were under-represented in our datasets. We therefore included a limited number ($n < 100$) of stations where these sediments had been observed and randomly assigned a sediment composition adhering to their class definitions (Folk, 1954). These pseudo-observations were used in the grain-size and dry bulk density datasets.

2.2 Predictors variables

We created a raster stack of predictor variables that we considered potentially relevant for predicting the response variables and that were available with (near) full coverage in the area of interest at a sufficiently high spatial resolution. The resolution that was finally chosen was 4 km, which translates to a map scale of approximately 1 : 8,000,000 according to a recommended formula in Hengl (2006). The raster stack was projected to the Lambert azimuthal equal area projection.

We included variables on seafloor terrain (bathymetry, topographic position, distance to nearest shoreline), ocean colour (chlorophyll-a, primary production and suspended particulate matter), biogeochemisty (surface partial pressure of CO_2, dissolved molecular oxygen of bottom water), sea ice concentration, bottom fishing intensity (swept area ratio), and oceanography (current speed, temperature, and salinity). Multi-annual statistics (mean, minimum, maximum, and range) were calculated for most predictors (Table S3).

3 Methods

3.1 Spatial predictions

3.1.1 Machine learning algorithms

We chose the random forest (RF) algorithm (Breiman, 2001) to spatially predict the response variables substrate type, depositional environment, and mud content. Further, we use the quantile regression forest (QRF) algorithm (Meinshausen, 2006) to make spatial predictions of the response variables dry bulk density, organic carbon content and ^{210}Pb-derived sediment accumulation rates. QRF can be seen as an extension of the RF algorithm, which has shown high predictive accuracy in several studies across various research domains (Huang et al., 2014; Mutanga et al., 2012; Oliveira et al., 2012; Prasad et al., 2006). RF can be used for both classification and regression modelling, while QRF deals only with regression tasks. RF is an ensemble technique that grows many trees and aggregates the majority class (classification) or conditional mean (regression) from each tree in a forest to make an ensemble prediction. QRF also returns the whole conditional distribution of the response variable, based on which other measures of central tendency (e.g., median) and of prediction uncertainty can be obtained. Following common practice in the global soil mapping community (Arrouays et al., 2014; Heuvelink, 2014), we used the 90 % prediction interval (PI90) as a measure of spatially explicit uncertainty. PI90 gives the range of values within which the true value is expected to occur nine times out of ten, with a one in 20 probability for each of the two tails (Arrouays et al., 2014). It is defined as

$$\boldsymbol{PI90 = q_{0.95} - q_{0.05}} \tag{1}$$

with q0.95 and q0.05 being the 0.95 and 0.05 quantiles of the distribution, respectively. We chose the median as a measure of central tendency, as the conditional distributions are most likely non-normal, and the median is not affected by extreme outliers.

3.1.2 Pre-processing

Prior to modelling, the predictor raster stack was cropped to the area of interest. Areas mapped as “Rock and boulders” in the substrate type model were excluded from further analysis, as we are only interested in the sedimentary environment. The datasets of the response variables organic carbon content and dry bulk density included information on depth below seabed. These datasets were filtered to only include records between 0 cm and 10 cm depth. The response data were averaged in those cases where more than one value was falling into a grid cell of the predictor stack.

3.1.3 Predictor variable selection

Although it is prudent to initially select a wide range of predictors, it is generally recommended to limit the number of predictors that are finally used for modelling. This is especially true when the number of records in the response data set is low. Variable selection can be achieved in different ways. Here we chose forward feature (variable) selection as implemented in the package CAST (Meyer et al., 2018). The algorithm first trains models based on all possible combinations of two predictor variables. The best combination is retained and tested for the best performance with a third variable. Additional variables are added until the performance stops improving. The model performance was calculated as R^2 using a spatial cross-validation scheme (see below). Prior to forward feature selection, a predictor variable pre-selection was executed to limit processing time. This pre-selection process initially only retained important variables that performed better than random variables using the Boruta algorithm (Kursa & Rudnicki, 2010). In the second step of the variable pre-selection, a de-correlation analysis was carried out to limit the collinearity. This was achieved with the *vifcor* function of the package usdm (Naimi et al., 2014). The function requires a correlation threshold and the predictor variables as input to calculate the variance inflation factor (VIF). The correlation threshold was stepwise decreased from 1 with a step size of 0.01 until the VIF was below 2.5 to avoid a problematic amount of collinearity (Johnston et al., 2018).

3.1.4 Model performance

Model performance needs to be estimated for model tuning, variable selection, and model validation. Model performance estimation is frequently based on k-fold cross validation, whereby the response data are split into k folds, a model is built on k – 1 folds, and validated against the fold which was not used for model building. This process is repeated k times. In standard, non-spatial machine learning applications, this k-fold split is performed randomly on the response data. However, this is not appropriate in the case of spatial data as spatial autocorrelation might lead to inflated estimates of model performance (Ploton et al., 2020; Roberts et al., 2017). Folds therefore need to be spatially separated and this was achieved with the function *cv_spatial* of the package blockCV (Valavi et al., 2019). Block size was initially determined by estimating the spatial autocorrelation range of the response data with the automap package (Hiemstra et al., 2009). The distance functions of the sample-to-sample, prediction-to-sample, and cross validation distances were plotted with the *plot_geodist* function of CAST (Meyer & Pebesma, 2021) and the block size altered by applying a multiplier to the spatial autocorrelation range until there was a visual agreement between the distance functions of the prediction-to-sample and cross validation distances.
The performance of the final regression models (mud content, dry bulk density, organic carbon content and sediment accumulation rate) was assessed based on the explained variance (R^2) and the root mean square error (RMSE). The performance of the classification models (Substrate type and Depositional environment) was assessed with the overall accuracy (Congalton, 1991) and the balanced error rate (BER, Luts et al., 2010), which is the average of the proportion of wrong classifications in each class, thereby accounting for class imbalances.

3.1.5 Area of applicability

Although it is technically possible to predict the response variable over the full extent of the predictor variables, such predictions might be unreliable where they extrapolate beyond the predictor variable space that has been captured by the model (Meyer & Pebesma, 2021, 2022). It has therefore been suggested to estimate the area of applicability (AOA) of a model, where the combination of predictor variables is similar to what the model has been trained with. This can be achieved with the *aoa* function of the package CAST (Meyer et al., 2023).

3.1.6 Qualitative evaluation

Additionally, we used expert judgement to evaluate whether the predicted patterns were reasonable by comparing them with existing maps and a general understanding of the involved processes and their products. Although such an assessment is qualitative and somewhat subjective, it is currently the only way to incorporate expert knowledge and we consider it an essential part of the mapping process.

3.2 Calculation of organic carbon stocks

Organic carbon stocks (OCS) are calculated by multiplying the predicted organic carbon contents (G) with the predicted dry bulk densities (ρ_d) and the sediment thickness (d = 0.1 m):

$$\boldsymbol{OCS}\ (\boldsymbol{kg\ m^{-2}}) = \frac{\boldsymbol{G}\ (\%)}{\mathbf{100}} \cdot \mathbf{1000} \cdot \boldsymbol{\rho_d}\ (\boldsymbol{g\ cm^{-3}}) \cdot \boldsymbol{d}\ (\mathrm{m}) \tag{2}$$

Calculations were carried out for the whole area and limited to the joint AOA of the organic carbon and dry bulk density models.

The total reservoir size mOC was calculated by summing OCS of all pixels and multiplying with the area of one pixel (A = 16,000,000 m^2):

$$\boldsymbol{m_{OC}(Tg)} = (\boldsymbol{A(m^2)} \cdot \sum \boldsymbol{OCS}\ (\boldsymbol{kg\ m^{-2}}))/\mathbf{1,000,000,000} \tag{3}$$

3.3 Calculation of organic carbon accumulation rates

Organic carbon accumulation rates (OCAR) are calculated by multiplying organic carbon contents (0 – 10 cm) with dry bulk densities and sediment accumulation rates (w):

$$\boldsymbol{OCAR}\ (\boldsymbol{g\ m^{-2}\ yr^{-1}}) = \frac{\boldsymbol{G}\ (\%)}{\mathbf{100}} \cdot \boldsymbol{\rho_d}\ (\boldsymbol{g\ cm^{-3}}) \cdot \boldsymbol{\omega}(\boldsymbol{cm\ yr^{-1}}) \cdot \mathbf{10,000} \tag{4}$$

Calculations were carried out for the whole area and limited to the joint AOA of the organic carbon, dry bulk density and sediment accumulation rate models.

The total mass of organic carbon that is accumulated annually (OCA) is calculated by summing OCAR of all pixels and multiplying with the area of one pixel (A = 16,000,000 m^2):

$$\boldsymbol{OCA}(\boldsymbol{Tg\ yr^{-1}}) = (\boldsymbol{A(m^2)} \cdot \sum \boldsymbol{OCAR}\ (\boldsymbol{g\ m^{-2}\ yr^{-1}}))/\mathbf{1,000,000,000,000} \tag{5}$$

3.4 Propagation of uncertainties

Uncertainties were propagated by taking the square root of the sum of squared relative uncertainties:

$$\boldsymbol{\delta OCS} = \boldsymbol{OCS} \cdot \sqrt{\left(\frac{\boldsymbol{\delta G}}{\boldsymbol{G}}\right)^{\mathbf{2}} + \left(\frac{\boldsymbol{\delta \rho_d}}{\boldsymbol{\rho_d}}\right)^{\mathbf{2}}} \tag{6}$$

$$\boldsymbol{\delta OCAR} = \boldsymbol{OCAR} \cdot \sqrt{\left(\frac{\boldsymbol{\delta G}}{\boldsymbol{G}}\right)^{\mathbf{2}} + \left(\frac{\boldsymbol{\delta \rho_d}}{\boldsymbol{\rho_d}}\right)^{\mathbf{2}} + \left(\frac{\boldsymbol{\delta \omega}}{\boldsymbol{\omega}}\right)^{\mathbf{2}}} \tag{7}$$

The symbol δ signifies the uncertainty of a quantity.

4 Results and discussion

4.1 Model Performance

The characteristics and performance indicators of the six spatial models are summarised in Table 2. It is important to stress that the performance indicators were derived in a spatial cross-validation scheme and were expected to be lower than those derived from random cross-validation, which was frequently employed in previous studies. Despite this, our model on organic carbon content explains 77% of the variance in the data. This is comparable to studies which did not employ spatial cross-validation (Atwood et al., 2020; Diesing et al., 2017; Lee et al., 2019). The mud content model had a similar R^2 value of 0.76, higher than those of previously published models (Mitchell et al., 2019; Stephens & Diesing, 2015; Wilson et al., 2018). The dry bulk density model explained 70% of the variance. This is, to our knowledge, the first published model on this seafloor sediment property. The model for sediment accumulation rates performed somewhat poorer, explaining 32% of the variance. Previous studies have shown that predicting sediment accumulation rates with machine learning can be challenging (e.g., Mitchell et al., 2021). However, based on a comparison with published maps (Bøe et al., 1996; de Haas et al., 1997; Pathirana et al., 2014) and our expert judgement, we conclude that the overall patterns of sediment accumulation (Fig. S6) are reasonable. The model on the depositional environment performed well with an overall accuracy of 81% and a balanced error rate of 0.28. The lower performance of the substrate type model might be attributable to the higher number of classes (eight vs three).

This is one of the first marine studies that employed the concept of the area of applicability (Meyer & Pebesma, 2021). All models had areas of applicability larger than 80% of the total area, two of them (substrate type and organic carbon content) even >90%. The resulting maps (Figures 2-3, S1-S6) are therefore applicable to at least 80% of the area of interest.

Table 2. Summary of the six models and their performance. Model types: RF- Random Forest; QRF – Quantile Regression Forest. BER – Balanced Error Rate. RMSE – Root Mean Squared Error. AOA – Area of Applicability.

Response variable	**Type**	**Unit**	**Number of samples**	**Number of predictors**	**Model**	**Accuracy**	**BER**	**RMSE**	**R^2**	**AOA (% of total area)**
Substrate type	categorical	-	23798	9	RF	0.59	0.53	-	-	91.22
Depositional environment	categorical	-	13305	9	RF	0.81	0.28	-	-	88.02
Mud content[1]	continuous	weight -%	4531	9	RF	-	-	1.456	0.76	81.53
Dry bulk density	continuous	g cm^{-3}	606	10	QRF	-	-	0.192	0.70	88.57
Organic carbon content	continuous	weight -%	697	8	QRF	-	-	0.339	0.77	91.32
Sediment accumulation rate	continuous	cm yr^{-1}	220	8	QRF	-	-	0.135	0.32	88.19

[1]Model information relates to the additive log-ratio model.

4.2 Substantial amounts of organic carbon are stored in continental margin sediments

Organic carbon stocks of the upper 0.1 m of seafloor sediments range between 0.11 and 3.34 kg m^{-2}, while the uncertainty varies between 0.21 and 4.04 kg m^{-2} (Figure 2). Stocks are lowest (<0.5 kg m^{-2}) on the North Sea shelf, shelf banks in the Norwegian Sea, along the shelf edge and slope foot and in parts of the southern Barents Sea. Conversely, stocks are highest (>2 kg m^{-2}) off the northern and western coasts of Svalbard and in a southwest-northeast oriented band from Spitsbergen Bank to Central Bank. However, the calculated stocks on Spitsbergen Bank lie outside the joint area of applicability of the organic carbon and dry bulk density models and might be unrealistic, as coarse sediments (Bjørlykke et al., 1978) and mobile bedforms (Bellec et al., 2019) are widespread on the bank (Figures S1 and S2). Interestingly, the highest stocks as described above are located north of the marginal ice zone (Figure 2). In the seasonally sea ice covered northern area, higher stocks could reflect a highly variable primary production regime with efficient vertical export and less recycling than in the southern Barents Sea. Indeed, measured accumulation rates of organic carbon here are more than twice as high as in the ice-free southern region (Faust et al., 2020) reflecting the modern ecosystem with higher primary productivity but lower vertical organic flux rates in the southern than in the northern Barents Sea.

In addition, sea-ice induced lateral transport and subsequent release of terrestrial organic carbon can further accelerate deposition of primary produced organic carbon in the marginal ice zone (Knies & Martinez, 2009). Shelf valleys tend to have higher organic carbon stocks than their surrounding areas. This contrast is particularly stark between the Norwegian Trough and the North Sea shelf, indicating that shelf sediments can act in distinctly different ways in the context of organic carbon processing (Diesing et al., 2021). Indeed, centres of organic carbon accumulation and oxidation (Bianchi et al., 2018) might lie in close proximity to each other.

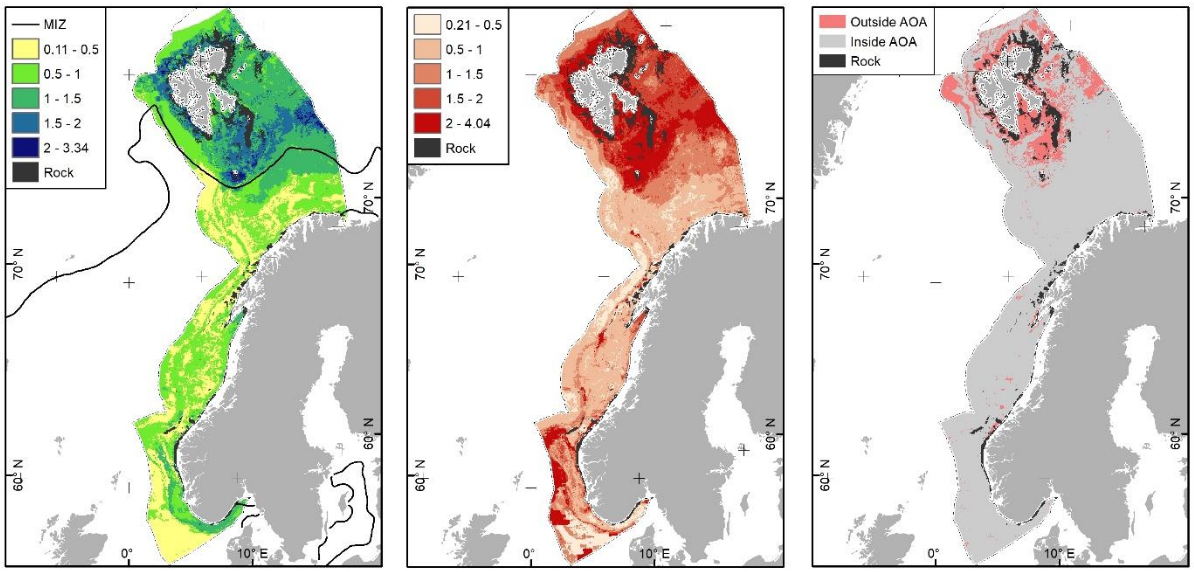

Figure 2. Organic carbon stocks of surficial (0 – 10 cm) sediments on the Norwegian continental margin. Stocks were calculated from predicted dry bulk densities (Figure S4) and organic carbon contents (Figure S5). Left - Estimated organic carbon stocks (kg C m^{-2}). MIZ – marginal ice zone based on Itkin et al. (2014). Centre – Prediction uncertainty (kg m^{-2}), expressed as the 90% prediction interval. Right – Joint area of applicability (AOA) of the models. Areas predicted as rock in the substrate type model (Figure S1) were excluded from the analysis.

The reservoir size of margin sediments in Norway was calculated to 1,002 ± 1,485 Tg C within the area of interest and 793 ± 1,152 Tg C within the joint area of applicability. By comparison, current best estimates of reservoir sizes in vegetated coastal ecosystems (salt marshes, eelgrass meadows and brown macroalgae) in the Nordic countries (Greenland, Iceland, Faroe Islands, Norway, Denmark, Sweden, and Finland) amount to 9.26 Tg C (Krause-Jensen et al., 2022). The organic carbon reservoir size of vegetated coastal ecosystems in Norway has been estimated to be 5 – 22 Tg C (Bartlett et al., 2020). Continental margin sediments thus store approximately two orders of magnitude more organic carbon than coastal vegetated ecosystems, even though we have only considered the upper 0.1 m of the sediment column while other estimates typically refer to the upper 1 m (Figure 3). Reservoir sizes of margin sediments might even be comparable to terrestrial ecosystems such as forest soils (1,240 – 1,830 Tg C) and wetlands (890 – 2,089 Tg C) in Norway (Bartlett et al., 2020). Despite the remaining uncertainties in the estimates, it would appear that continental margin sediments store substantial amounts of organic carbon and have so far been overlooked in the context of Blue Carbon.

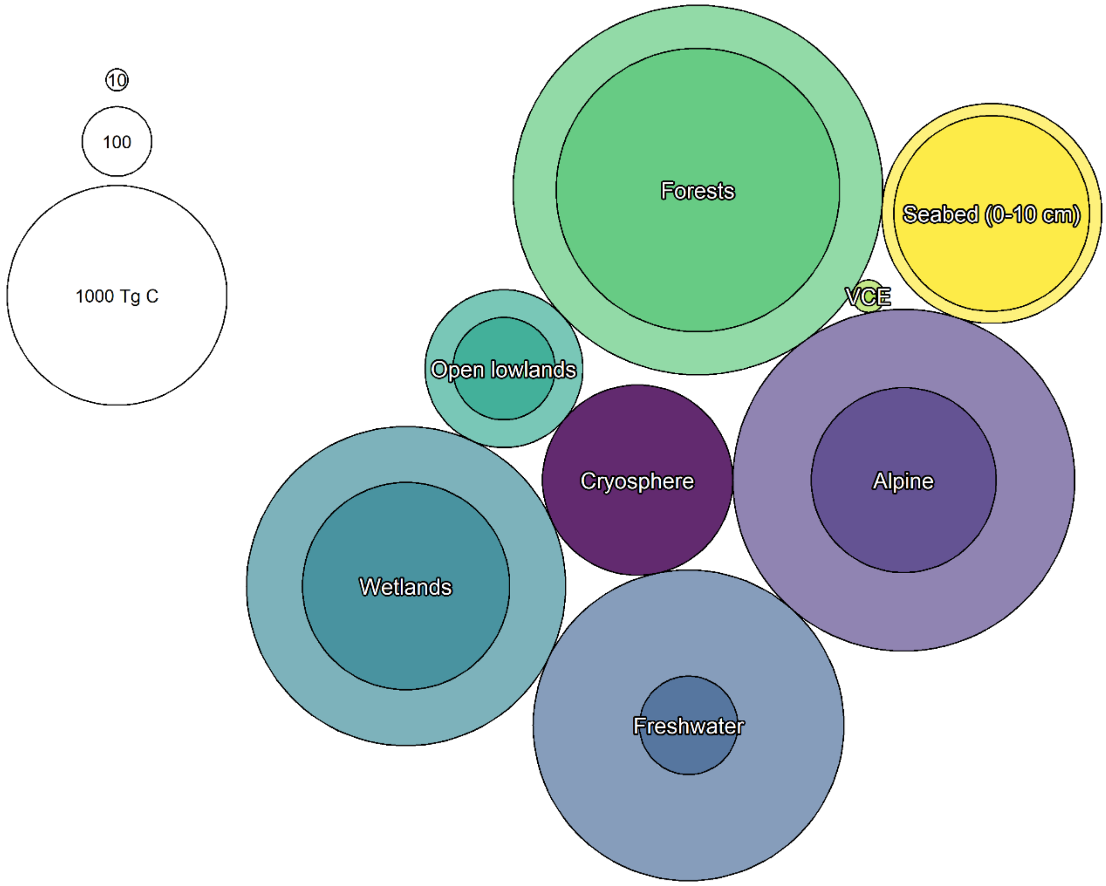

Figure 3. Comparison of various organic carbon reservoir sizes in Norway: Surficial seabed sediments harbour between 793 Tg C (inside the AOA) and 1002 Tg C (inside and outside AOA). The reservoir size of vegetated coastal ecosystems (VCE) is much smaller (5 – 22 Tg C). Surficial seabed sediments have organic carbon reservoir sizes comparable to several terrestrial ecosystems such as wetlands and forests. Inner circles depict lower limit and outer circles upper limit of the estimated range of values. Data on Blue Carbon and terrestrial ecosystems are taken from Bartlett et al. (2020).

4.3 Complex patterns of organic carbon accumulation

As we used ^{210}Pb-derived sediment accumulation rates, the following estimates refer to accumulation over the last 100 - 150 yr based on its half-life of 22.2 yr and an integration time of approximately five to seven times the half-life (Goldberg, 1963).

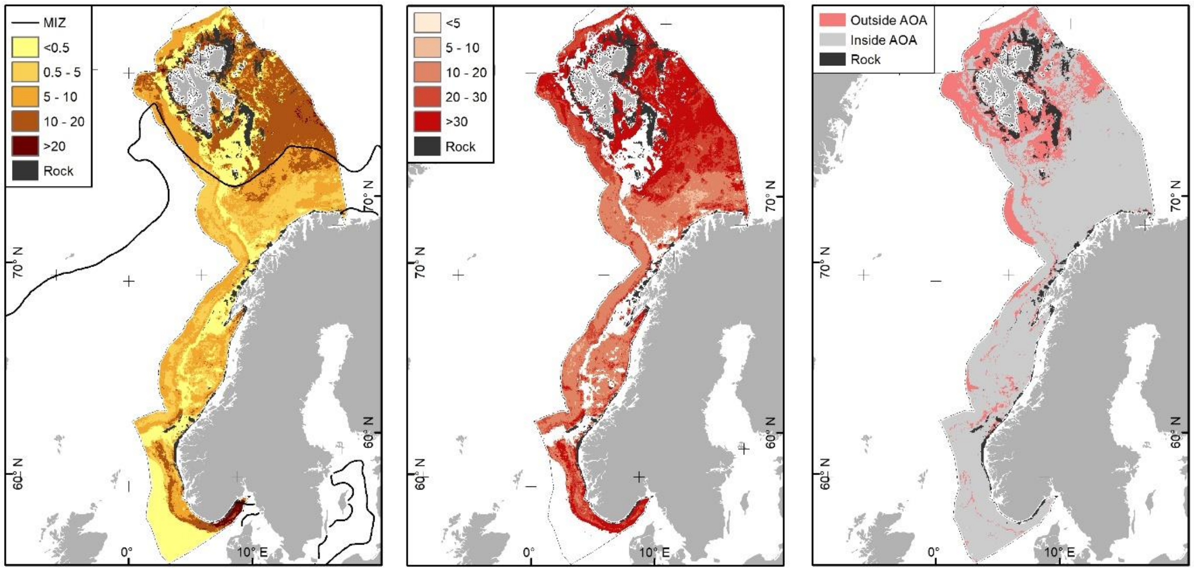

Figure 4. Organic carbon accumulation rates on the Norwegian continental margin. Organic carbon accumulation rates were calculated from organic carbon stocks of surficial (0 – 10 cm) sediments (Figure 2) and sediment accumulation rates (Figure S6). Left - Estimated organic carbon accumulation rates (g C m^{-2} yr^{-1}). MIZ – marginal ice zone based on Itkin et al. (2014). Centre – Prediction uncertainty (g C m^{-2} yr^{-1}), expressed as the 90% prediction interval. Note that the uncertainty is not defined in areas with sedimentation rates of 0 cm yr^{-1} (see equation 7). Right – Joint area of applicability of the models. Areas predicted as rock in the substrate type model (Figure S1) were excluded from the analysis.

Organic carbon accumulation rates range from 0.0 to 106.4 g C m^{-2} yr^{-1}, with uncertainties varying between 2.4 and 264.7 g C m^{-2} yr^{-1} (Figure 4). Zero-accumulation of organic carbon is linked to the North Sea shelf, the shelf break, shelf banks in the Norwegian Sea, and Spitsbergen Bank, the latter in agreement with Pathirana et al. (2014). The main hotspot of organic carbon accumulation is to be found in the inner part of the Norwegian Trough in the Skagerrak. Additionally, elevated rates of organic carbon accumulation are widespread in the Barents Sea north of the marginal ice zone. However, calculated organic carbon accumulation rates lie outside the joint area of applicability of the organic carbon, dry bulk density and sediment accumulation models around Svalbard and on Spitsbergen Bank. Again, geomorphology acts as a major driver of the patterns of organic carbon accumulation. Depressions like shelf valleys act as centres of organic carbon accumulation due to high sedimentation rates (Figure S6), while shallow banks and plateaus show no accumulation at all due to their erosional character (Figure S2). The shelf edge shows no accumulation of organic carbon due to relatively strong currents preventing sediments and organic carbon from long-term accumulation. Conversely, the slope and upper part of the abyss are places of organic carbon accumulation. These patterns are also reflected in the mean organic carbon accumulation rates of geomorphological units: Mean rates are lowest on the shallow continental shelf (2.24 g C m^{-2} yr^{-1}), which includes banks and plateaus, and highest in shelf valleys (8.23 g C m^{-2} yr^{-1}), where they are nearly four times higher than on the inner shelf (Figure 5a). Elevated mean rates are also to be found on the deep continental shelf (5.33 g C m^{-2} yr^{-1}), while slopes and the abyss exhibit moderate mean rates of 2.92 g C m^{-2} yr^{-1} and 3.15 g C m^{-2} yr^{-1}, respectively.

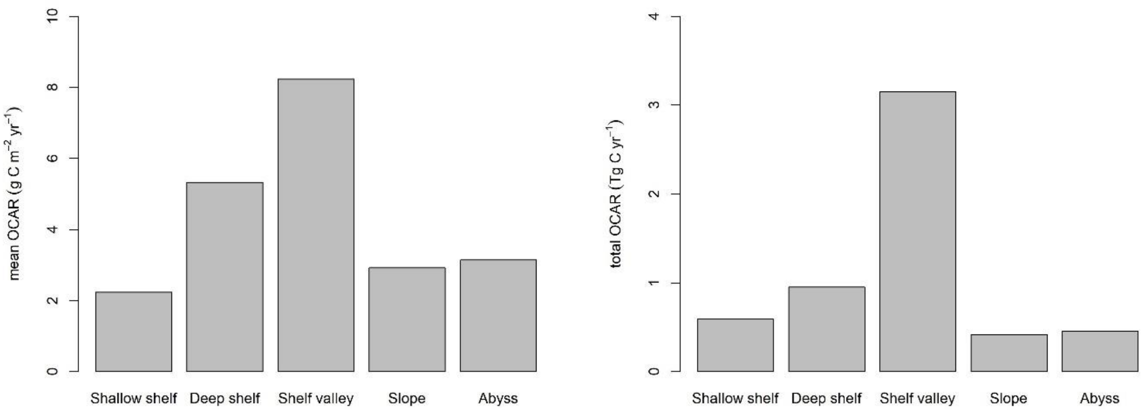

Figure 5. Organic carbon accumulation rates of the geomorphological units as shown in Figure 1. Left – Mean organic carbon accumulation rates averaged over the five morphological units. Right – Total organic carbon accumulation, i.e., mean rates multiplied by area.

Aggregated over the area of interest, the sediments of the Norwegian continental margin accumulate 7.5 ± 24.7 Tg C yr^{-1}. Restricted to the joint area of applicability, organic carbon accumulation amounts to 5.6 ± 18.1 Tg C yr^{-1}. For comparison, coastal vegetated ecosystems might accumulate 0.55 Tg C yr^{-1} in the Nordic countries (Krause-Jensen et al., 2022) and 0.25 – 0.37 Tg C yr^{-1} in Norway (Bartlett et al., 2020). Expressed in equivalents of CO_2, Norwegian margin sediments accumulate 20.6 Tg CO_2-eq per year within the joint area of applicability. This is equivalent to 42% of Norway's greenhouse gas emissions of 48.9 Tg CO_2-eq in 2022 (SSB, 2023).
More than half of the accumulation of organic carbon is happening in shelf valleys (Figure 5b) due to their high accumulation rates per unit area (Figure 5a) and the large areas they occupy on the Norwegian continental margin (Figure 1), amounting to 388,288 km^2. Shelf valleys are therefore centres of organic carbon accumulation on the Norwegian continental margin. Most of these geomorphological features are of glacial origin and could also be described as glacial troughs attributed to glacial erosion during the Pleistocene ice ages. Globally, glacial troughs are found on the formerly glaciated continental margins of North America, Eurasia, south America, and Antarctica, covering 3.66 million km^2 of the seabed (Harris et al., 2014). If we assume that the rate of organic carbon accumulation in shelf valleys of 8.23 g C m^{-2} yr^{-1}we derived is representative for glacial troughs globally, then these geomorphological features might accumulate 30 Tg C yr^{-1}, which is comparable to fjords (21 – 25 Tg C/yr; Smith et al., 2015), seagrass meadows (14.7 - 27.4 Tg C/yr; Duarte et al., 2005; Taillardat et al., 2018), mangroves (13.5 - 26.1 Tg C/yr; Alongi, 2012; Breithaupt et al., 2012; Taillardat et al., 2018), and saltmarshes (10.1 - 10.2 Tg C/yr; Ouyang & Lee, 2014; Taillardat et al., 2018). Although our global estimate is currently tentative, it points to a hitherto overlooked environment with high potential for organic carbon accumulation.

4.4 Towards a global map of organic carbon accumulation rates

Previous estimates of organic carbon burial in seafloor sediments of the global ocean have frequently been non-spatial and only Burdige (2007) considered that large parts of continental

margins do not accumulate sediment and organic carbon (de Haas et al., 2002). Moreover, assumptions about how much organic carbon that is accumulated at the seafloor gets eventually buried are frequently very general. For example, Berner (1982) assumed a preservation rate of 80% globally. Estimated organic carbon fluxes based on satellite data (Dunne et al., 2007; Muller-Karger et al., 2005) gave spatially explicit results, but also had to make assumptions about the burial efficiency, e.g., Muller-Karger et al. (2005) assumed burial efficiencies of 30% in the deep sea and 10% on margins. Moreover, such studies were not able to resolve the spatial complexities of continental margin processes, as they implicitly assumed a static ocean where organic matter sinks to the seafloor and resuspension, erosion and transport had little effect. Consequently, these studies estimated high rates of organic carbon burial across all margins. Because of the vague definition of organic carbon burial (see the discrepancies between the values of burial efficiency cited above and Bradley et al. (2022)), we decided to estimate organic carbon accumulation rates instead. These are representative of the last 100 to 150 years, i.e., the time interval since the start of the industrial revolution and the increase of anthropogenic CO_2 emissions due to the burning of fossil fuels. We were also able to account for the complex nature of the Norwegian continental margin in terms of sediment erosion and deposition because the depositional environment is being mapped as part of the Mareano programme.
Unlike organic carbon content (Lee et al., 2019) and stocks (Atwood et al., 2020), organic carbon accumulation rates have not been mapped globally with machine learning approaches. To do so will require a) data on organic carbon content, dry bulk density and sediment accumulation rates of sufficient quality and quantity, b) relevant predictor variables of global coverage and sufficient resolution, and c) spatial models that take into account the complex nature of continental margins, where centres of organic carbon accumulation and cycling might be found in close proximity to each other (Diesing et al., 2021; de Haas et al., 2002). While progress has been made to make relevant response (Felden et al., 2023; Paradis et al., 2023) and predictor variables (Assis et al., 2018) available, there are still several obstacles that need to be overcome. We consider the lack of a global map of the depositional environment as the main obstacle on a path towards a global map of organic carbon accumulation rates. Burdige (2007) used Emery's (1968) map of relict sediments on the continental shelves of the global ocean as a proxy. However, this map does not exist electronically, might be outdated by now and is not explicitly depicting the depositional environment. The first task would therefore be to predict the depositional environment on continental margins globally.

5 Conclusions

We spatially predicted dry bulk density, organic carbon content and sediment accumulation rates of surface sediments on the continental margin of Norway to estimate organic carbon stocks and accumulation rates. Organic carbon reservoirs are two orders of magnitude larger than those of vegetated coastal ecosystems in Norway, even if we only considered the upper ten centimetres of the sediment column. Rates of organic carbon accumulation are spatially highly variable and highest in shelf valleys of mostly glacial origin. Considering the global extension of glacial troughs in the global ocean, these geomorphologic features might be accumulating as much organic carbon as fjords, seagrass meadows, mangroves, and saltmarshes. Global spatial predictions of sediment and organic carbon accumulation rates are required for a better understanding of the role of margin sediments in the carbon cycle and to evaluate whether continental margin sediments constitute actionable Blue Carbon ecosystems.

Acknowledgments

This work was funded by the Norwegian seabed mapping programme Mareano. JK received support from the Research Council of Norway (grant # 332635).

Conflict of interest

The authors declare no conflict of interest.

Open Research

Calculated organic carbon stocks and accumulation rates and the related uncertainties and areas of applicability are available from PANGAEA: [*Insert doi when minted*]
Input (response and predictor variables) and output data of the six spatial models are available at Zenodo. The R codes developed to spatially predict the response variables are available at GitHub.

NB! Data on Zenodo and PANGAEA have been created but not yet published. The datasets have been made available for peer review.

Variable	Input data	Output data	R workflow
Substrate type	https://doi.org/10.5281/zenodo.10040165	https://doi.org/10.5281/zenodo.10053285	https://github.com/diesing-ngu/GrainSizeReg
Depositional environment	https://doi.org/10.5281/zenodo.10040720	https://doi.org/10.5281/zenodo.10053457	https://github.com/diesing-ngu/SedEnv
Mud content	https://doi.org/10.5281/zenodo.10057143	https://doi.org/10.5281/zenodo.10057207	https://github.com/diesing-ngu/GSMgrids
Dry bulk density	https://doi.org/10.5281/zenodo.10057726	https://doi.org/10.5281/zenodo.10057750	https://github.com/diesing-ngu/DBD
Organic carbon content	https://doi.org/10.5281/zenodo.10058434	https://doi.org/10.5281/zenodo.10058520	https://github.com/diesing-ngu/TOC
Sediment accumulation rate	https://doi.org/10.5281/zenodo.10061180	https://doi.org/10.5281/zenodo.10062619	https://github.com/diesing-ngu/SedRates

References

Alongi, D. M. (2012). Carbon sequestration in mangrove forests. *Carbon Management*, *3*(3), 313–322. https://doi.org/10.4155/cmt.12.20

Arrouays, D., Grundy, M. G., Hartemink, A. E., Hempel, J. W., Heuvelink, G. B. M., Hong, S. Y., et al. (2014). Chapter Three - GlobalSoilMap: Toward a Fine-Resolution Global Grid of Soil Properties. In D. L. Sparks (Ed.) (Vol. 125, pp. 93–134). Academic Press. https://doi.org/https://doi.org/10.1016/B978-0-12-800137-0.00003-0

Assis, J., Tyberghein, L., Bosch, S., Verbruggen, H., Serrão, E. A., & De Clerck, O. (2018). Bio-ORACLE v2.0: Extending marine data layers for bioclimatic modelling. *Global Ecology and Biogeography*, *27*(3), 277–284. https://doi.org/10.1111/geb.12693

Atwood, T. B., Witt, A., Mayorga, J., Hammill, E., & Sala, E. (2020). Global Patterns in Marine Sediment Carbon Stocks. *Frontiers in Marine Science*, *7*, 165. https://doi.org/10.3389/fmars.2020.00165

Bartlett, J., Rusch, G. M., Kyrkjeeide, M. O., Sandvik, H., & Nordén, J. (2020). Carbon storage in Norwegian ecosystems (revised edition). *NINA Report*, *1774b*. Retrieved from https://hdl.handle.net/11250/2655580

Bellec, V. K., Bøe, R., Bjarnadóttir, L. R., Albretsen, J., Dolan, M., Chand, S., et al. (2019). Sandbanks, sandwaves and megaripples on Spitsbergenbanken, Barents Sea. *Marine Geology*, *416*, 105998. https://doi.org/https://doi.org/10.1016/j.margeo.2019.105998

Berner, R. A. (1982). Burial of organic carbon and pyrite sulfur in the modern ocean: Its geochemical and environmental significance. *American Journal of Science*, *282*, 451–473. https://doi.org/10.2475/ajs.282.4.451

Berner, R. A. (2003). The long-term carbon cycle, fossil fuels and atmospheric composition. *Nature*, *426*, 323. Retrieved from https://doi.org/10.1038/nature02131

Bianchi, T. S., Cui, X., Blair, N. E., Burdige, D. J., Eglinton, T. I., & Galy, V. (2018). Centers of organic carbon burial and oxidation at the land-ocean interface. *Organic Geochemistry*, *115*, 138–155. https://doi.org/https://doi.org/10.1016/j.orggeochem.2017.09.008

Bjørlykke, K., Bue, B., & Elverhøi, A. (1978). Quaternary sediments in the northwestern part of the Barents Sea and their relation to the underlying Mesozoic bedrock. *Sedimentology*, *25*(2), 227–246. https://doi.org/https://doi.org/10.1111/j.1365-3091.1978.tb00310.x

Bøe, R., Rise, L., Thorsnes, T., de Haas, H., Sæther, O. M., & Kunzendorf, H. (1996). Sea-bed sediments and sediment accumulation rates in the Norwegian part of the Skagerrak. *NGU Bulletin*, *430*, 75–84.

Bradley, J. A., Hülse, D., LaRowe, D. E., & Arndt, S. (2022). Transfer efficiency of organic carbon in marine sediments. *Nature Communications*, *13*(1), 7297. https://doi.org/10.1038/s41467-022-35112-9

Breiman, L. (2001). Random Forests. *Machine Learning*, *45*, 5–32. https://doi.org/https://doi.org/10.1023/A:1010933404324

Breithaupt, J. L., Smoak, J. M., Smith III, T. J., Sanders, C. J., & Hoare, A. (2012). Organic carbon burial rates in mangrove sediments: Strengthening the global budget. *Global Biogeochemical Cycles*, *26*(3). https://doi.org/https://doi.org/10.1029/2012GB004375

Burdige, D. J. (2007). Preservation of Organic Matter in Marine Sediments: Controls, Mechanisms, and an Imbalance in Sediment Organic Carbon Budgets? *Chemical Reviews*, *107*(2), 467–485. https://doi.org/10.1021/cr050347q

Congalton, R. G. (1991). A review of assessing the accuracy of classifications of remotely sensed data. *Remote Sensing of Environment*, *37*(1), 35–46. Retrieved from http://www.sciencedirect.com/science/article/pii/003442579190048B

Diesing, M., Kröger, S., Parker, R., Jenkins, C., Mason, C., & Weston, K. (2017). Predicting the standing stock of organic carbon in surface sediments of the North–West European continental shelf. *Biogeochemistry*, *135*(1–2), 183–200. https://doi.org/10.1007/s10533-017-0310-4

Diesing, M., Thorsnes, T., & Bjarnadóttir, L. R. (2021). Organic carbon densities and accumulation rates in surface sediments of the North Sea and Skagerrak. *Biogeosciences*, *18*(6), 2139–2160. https://doi.org/10.5194/bg-18-2139-2021

DNV. (2023). Environmental Monitoring database (MOD) DNV. https://doi.org/https://doi.org/10.15468/q8qykg

Duarte, C. M., Middelburg, J. J., & Caraco, N. (2005). Major role of marine vegetation on the oceanic carbon cycle. *Biogeosciences*, *2*(1), 1–8. https://doi.org/10.5194/bg-2-1-2005

Duarte, C. M., Losada, I. J., Hendriks, I. E., Mazarrasa, I., & Marbà, N. (2013). The role of coastal plant communities for climate change mitigation and adaptation. *Nature Climate Change*, *3*(11), 961–968. https://doi.org/10.1038/nclimate1970

Dunne, J. P., Sarmiento, J. L., & Gnanadesikan, A. (2007). A synthesis of global particle export from the surface ocean and cycling through the ocean interior and on the seafloor. *Global Biogeochemical Cycles*, *21*(4). https://doi.org/https://doi.org/10.1029/2006GB002907

Emery, K. O. (1968). Relict sediments on continental shelves of world. *American Association of Petroleum Geologists Bulletin*, *52*(3), 445–464.

Faust, J. C., Stevenson, M. A., Abbott, G. D., Knies, J., Tessin, A., Mannion, I., et al. (2020). Does Arctic warming reduce preservation of organic matter in Barents Sea sediments? *Philosophical Transactions of the Royal Society A: Mathematical, Physical and Engineering Sciences*, *378*(2181), 20190364. https://doi.org/10.1098/rsta.2019.0364

Felden, J., Möller, L., Schindler, U., Huber, R., Schumacher, S., Koppe, R., et al. (2023). PANGAEA - Data Publisher for Earth & Environmental Science. *Scientific Data*, *10*(1), 347. https://doi.org/10.1038/s41597-023-02269-x

Folk, R. L. (1954). The distinction between grain size and mineral composition in sedimentary-rock nomenclature. *Journal of Geology*, *62*, 344–359.

GEBCO Bathymetric Compilation Group. (2019). The GEBCO_2019 Grid - a continuous terrain model of the global oceans and land. https://doi.org/10.5285/836f016a-33be-6ddc-e053-6c86abc0788e

Goldberg, E. D. (1963). Geochronology with Pb-210. In *Radioactive Dating. Proceedings of the Symposium on Radioactive Dating Held by the International Atomic Energy Agency in Co-operation with the Joint Commission on Applied Radioactivity* (pp. 121–131). Athens.

de Haas, H., Boer, W., & van Weering, T. C. E. (1997). Recent sedimentation and organic carbon burial in a shelf sea: the North Sea. *Marine Geology*, *144*, 131–146. https://doi.org/10.1016/S0025-3227(97)00082-0 de Haas, H., van Weering, T. C. E., & de Stigter, H. (2002). Organic carbon in shelf seas: sinks or sources, processes and products. *Continental Shelf Research*, *22*(5), 691–717. https://doi.org/10.1016/S0278-4343(01)00093-0

Harris, P. T., Macmillan-Lawler, M., Rupp, J., & Baker, E. K. (2014). Geomorphology of the oceans. *Marine Geology*, *352*, 4–24. https://doi.org/10.1016/j.margeo.2014.01.011

Hedges, J. I., & Keil, R. G. (1995). Sedimentary organic matter preservation: an assessment and speculative synthesis. *Marine Chemistry*, *49*(2–3), 81–115. https://doi.org/10.1016/0304-4203(95)00008-F

Hengl, T. (2006). Finding the right pixel size. *COMPUTERS & GEOSCIENCES*, *32*, 1283–1298.

Hengl, T., de Jesus, J., Heuvelink, G. B. M., Ruiperez Gonzalez, M., Kilibarda, M., Blagotić, A., et al. (2017). SoilGrids250m: Global gridded soil information based on machine learning. *PLOS ONE*, *12*(2), 1–40. https://doi.org/10.1371/journal.pone.0169748

Heuvelink, G. B. M. (2014). Uncertainty quantification of GlobalSoilMap products. Retrieved from https://api.semanticscholar.org/CorpusID:132005407

Hiemstra, P. H., Pebesma, E. J., Twenhöfel, C. J. W., & Heuvelink, G. B. M. (2009). Real-time automatic interpolation of ambient gamma dose rates from the Dutch radioactivity monitoring network. *Computers & Geosciences*, *35*(8), 1711–1721. https://doi.org/https://doi.org/10.1016/j.cageo.2008.10.011

Howard, J., Sutton-Grier, A. E., Smart, L. S., Lopes, C. C., Hamilton, J., Kleypas, J., et al. (2023). Blue carbon pathways for climate mitigation: Known, emerging and unlikely. *Marine Policy*, *156*, 105788. https://doi.org/https://doi.org/10.1016/j.marpol.2023.105788

Huang, Z., Siwabessy, J., Nichol, S. L., & Brooke, B. P. (2014). Predictive mapping of seabed substrata using high-resolution multibeam sonar data: A case study from a shelf with complex geomorphology. *Marine Geology*, *357*, 37–52. Retrieved from http://www.sciencedirect.com/science/article/pii/S0025322714002205

Hunt, C., Demšar, U., Dove, D., Smeaton, C., Cooper, R., & Austin, W. E. N. (2020). Quantifying Marine Sedimentary Carbon: A New Spatial Analysis Approach Using Seafloor Acoustics, Imagery, and Ground-Truthing Data in Scotland. *Frontiers in Marine Science*, *7*, 588. https://doi.org/10.3389/fmars.2020.00588

Itkin, M., Konig, M., Spreen, G., & Vongraven, D. (2014). Arctic sea ice frequency with maximum and minimum extentw. https://doi.org/10.21334/npolar.2014.a89b2682

Jenkins, C. (2005). Summary of the onCALCULATION methods used in dbSEABED. Retrieved September 2, 2016, from http://pubs.usgs.gov/ds/2006/146/docs/onCALCULATION.pdf

Jenkins, C. (2018). Sediment Accumulation Rates For the Mississippi Delta Region: a Time-interval Synthesis. *Journal of Sedimentary Research*, *88*(2), 301–309. https://doi.org/10.2110/jsr.2018.15

Johnston, R., Jones, K., & Manley, D. (2018). Confounding and collinearity in regression analysis: a cautionary tale and an alternative procedure, illustrated by studies of British voting behaviour. *Quality & Quantity*, *52*(4), 1957–1976. https://doi.org/10.1007/s11135-017-0584-6

Keil, R. (2017). Anthropogenic Forcing of Carbonate and Organic Carbon Preservation in Marine Sediments. *Annual Review of Marine Science*, *9*(1), 151–172. https://doi.org/10.1146/annurev-marine-010816-060724

Knies, J., & Martinez, P. (2009). Organic matter sedimentation in the western Barents Sea region: Terrestrial and marine contribution based on isotopic composition and organic nitrogen content. *Norwegian Journal of Geology*, *89*, 79–89.

Krause-Jensen, D., Gundersen, H., Björk, M., Gullström, M., Dahl, M., Asplund, M. E., et al. (2022). Nordic Blue Carbon Ecosystems: Status and Outlook. *Frontiers in Marine Science*, *9*. https://doi.org/10.3389/fmars.2022.847544

Kursa, M. B., & Rudnicki, W. R. (2010). Feature Selection with the **Boruta** Package. *Journal of Statistical Software*, *36*(11), 1–13. https://doi.org/10.18637/jss.v036.i11

Lee, T. R., Wood, W. T., & Phrampus, B. J. (2019). A Machine Learning (kNN) Approach to Predicting Global Seafloor Total Organic Carbon. *Global Biogeochemical Cycles*, *33*(1), 37–46. https://doi.org/10.1029/2018GB005992

Legge, O., Johnson, M., Hicks, N., Jickells, T., Diesing, M., Aldridge, J., et al. (2020). Carbon on the Northwest European Shelf: Contemporary Budget and Future Influences. *Frontiers in Marine Science*, *7*, 143. https://doi.org/10.3389/fmars.2020.00143

Lovelock, C. E., & Duarte, C. M. (2019). Dimensions of Blue Carbon and emerging perspectives. *Biology Letters*, *15*(3), 20180781. https://doi.org/10.1098/rsbl.2018.0781

Luts, J., Ojeda, F., Plas, R., Van De Moor, B., De Huffel, S., & Van Suykens, J. A. K. (2010). A tutorial on support vector machine-based methods for classification problems in chemometrics. *Analytica Chimica Acta*, *665*(2), 129–145.

Martín-Fernandéz, J. A., & Thió-Henestrosa, S. (2006). Rounded zeros: some practical aspects for compositional data. In A. Buccianti, G. Mateu-Figueras, & V. Pawlowsky- Glahn (Eds.), *Compositional Data Analysis in the Geosciences: From Theory to Practice* (Vol. 264, pp. 191–201). Geological Society of London.
Meinshausen, N. (2006). Quantile Regression Forests. *Journal of Machine Learning Research*, *7*, 983–999.
Meyer, H., & Pebesma, E. (2021). Predicting into unknown space? Estimating the area of applicability of spatial prediction models. *Methods in Ecology and Evolution*, *12*(9), 1620–1633. https://doi.org/https://doi.org/10.1111/2041-210X.13650
Meyer, H., & Pebesma, E. (2022). Machine learning-based global maps of ecological variables and the challenge of assessing them. *Nature Communications*, *13*(1), 2208. https://doi.org/10.1038/s41467-022-29838-9
Meyer, H., Reudenbach, C., Hengl, T., Katurji, M., & Nauss, T. (2018). Improving performance of spatio-temporal machine learning models using forward feature selection and target-oriented validation. *Environmental Modelling & Software*, *101*, 1–9. https://doi.org/https://doi.org/10.1016/j.envsoft.2017.12.001
Meyer, H., Mila, C., Ludwig, M., & Linnenbrink, J. (2023). CAST: “caret” applications for Spatial-Temporal Models. https://github.com/HannaMeyer/CAST. Retrieved from https://github.com/HannaMeyer/CAST
Mitchell, P. J., Aldridge, J., & Diesing, M. (2019). Legacy data: How decades of seabed sampling can produce robust predictions and versatile products. *Geosciences (Switzerland)*. https://doi.org/10.3390/geosciences9040182
Mitchell, P. J., Spence, M. A., Aldridge, J., Kotilainen, A. T., & Diesing, M. (2021). Sedimentation rates in the Baltic Sea: A machine learning approach. *Continental Shelf Research*, *214*, 104325. https://doi.org/https://doi.org/10.1016/j.csr.2020.104325
Muller-Karger, F. E., Varela, R., Thunell, R., Luerssen, R., Hu, C., & Walsh, J. J. (2005). The importance of continental margins in the global carbon cycle. *Geophysical Research Letters*, *32*(1). https://doi.org/https://doi.org/10.1029/2004GL021346
Mutanga, O., Adam, E., & Cho, M. A. (2012). High density biomass estimation for wetland vegetation using WorldView-2 imagery and random forest regression algorithm. *International Journal of Applied Earth Observation and Geoinformation*, *18*, 399–406. https://doi.org/10.1016/j.jag.2012.03.012
Naimi, B., Hamm, N. A. S., Groen, T. A., Skidmore, A. K., & Toxopeus, A. G. (2014). Where is positional uncertainty a problem for species distribution modelling? *Ecography*, *37*(2), 191–203. https://doi.org/https://doi.org/10.1111/j.1600-0587.2013.00205.x
Nellemann, C., Corcoran, E., Duarte, C. M., Valdés, L., De Young, C., Fonseca, L., & Grimsditch, G. (2009). *Blue Carbon: The Role of Healthy Oceans in Binding Carbon: A Rapid Response Assessment*. *Environment*.
Oliveira, S., Oehler, F., San-Miguel-Ayanz, J., Camia, A., & Pereira, J. M. C. (2012). Modeling spatial patterns of fire occurrence in Mediterranean Europe using Multiple Regression and Random Forest. *Forest Ecology and Management*, *275*, 117–129. https://doi.org/10.1016/j.foreco.2012.03.003
Ouyang, X., & Lee, S. Y. (2014). Updated estimates of carbon accumulation rates in coastal marsh sediments. *Biogeosciences*, *11*(18), 5057–5071. https://doi.org/10.5194/bg-11-5057-2014
Paradis, S., Nakajima, K., der Voort, T. S., Gies, H., Wildberger, A., Blattmann, T. M., et al. (2023). The Modern Ocean Sediment Archive and Inventory of Carbon (MOSAIC): version 2.0. *Earth System Science Data*, *15*(9), 4105–4125. https://doi.org/10.5194/essd-15-4105-2023
Pathirana, I., Knies, J., Felix, M., & Mann, U. (2014). Towards an improved organic carbon budget for the western Barents Sea shelf. *Climate of the Past*, *10*(2), 569–587. https://doi.org/10.5194/cp-10-569-2014
Pawlowsky-Glahn, V., & Olea, R. A. (2004). *Geostatistical Analysis of Compositional Data*. New York: Oxford University Press.
Ploton, P., Mortier, F., Réjou-Méchain, M., Barbier, N., Picard, N., Rossi, V., et al. (2020). Spatial validation reveals poor predictive performance of large-scale ecological mapping models. *Nature Communications*, *11*(1), 4540. https://doi.org/10.1038/s41467-020-18321-y
Prasad, A. M., Iverson, L. R., & Liaw, A. (2006). Newer classification and regression tree techniques: Bagging and random forests for ecological prediction. *Ecosystems*, *9*(2), 181–199. https://doi.org/10.1007/s10021-005-0054-1
Roberts, D. R., Bahn, V., Ciuti, S., Boyce, M. S., Elith, J., Guillera-Arroita, G., et al. (2017). Cross-validation strategies for data with temporal, spatial, hierarchical, or phylogenetic structure. *Ecography*, *40*(8), 913–929. https://doi.org/10.1111/ecog.02881
Smeaton, C., Hunt, C. A., Turrell, W. R., & Austin, W. E. N. (2021). Marine Sedimentary Carbon Stocks of the United Kingdom’s Exclusive Economic Zone. *Frontiers in Earth Science*, *9*, 50. https://doi.org/10.3389/feart.2021.593324

Smith, R. W., Bianchi, T. S., Allison, M., Savage, C., & Galy, V. (2015). High rates of organic carbon burial in fjord sediments globally. *Nature Geoscience*, *8*(6), 450–453. https://doi.org/10.1038/NGEO2421

SSB. (2023). Emissions to air. Retrieved November 2, 2023, from https://www.ssb.no/en/natur-og-miljo/forurensing-og-klima/statistikk/utslipp-til-luft

Stephens, D., & Diesing, M. (2015). Towards quantitative spatial models of seabed sediment composition. *PLoS ONE*, *10*(11), e0142502. https://doi.org/10.1371/journal.pone.0142502

Taillardat, P., Friess, D. A., & Lupascu, M. (2018). Mangrove blue carbon strategies for climate change mitigation are most effective at the national scale. *Biology Letters*, *14*(10), 20180251. https://doi.org/10.1098/rsbl.2018.0251

Valavi, R., Elith, J., Lahoz-Monfort, J. J., & Guillera-Arroita, G. (2019). blockCV: An r package for generating spatially or environmentally separated folds for k-fold cross-validation of species distribution models. *Methods in Ecology and Evolution*, *10*(2), 225–232. https://doi.org/10.1111/2041-210X.13107

van der Voort, T. S., Blattmann, T. M., Usman, M., Montluçon, D., Loeffler, T., Tavagna, M. L., et al. (2020). MOSAIC (Modern Ocean Sediment Archive and Inventory of Carbon): A (radio)carbon-centric database for seafloor surficial sediments. *Earth System Science Data Discussions*, *2020*, 1–27. https://doi.org/10.5194/essd-2020-199

Wilson, R. J., Speirs, D. C., Sabatino, A., & Heath, M. R. (2018). A synthetic map of the north-west European Shelf sedimentary environment for applications in marine science. *Earth System Science Data*, *10*(1), 109–130. https://doi.org/10.5194/essd-10-109-2018

AGU Advances

Supporting Information for

Organic Carbon Stocks and Accumulation Rates in Surface Sediments of the Norwegian Continental Margin

Markus Diesing[1], Sarah Paradis[2], Henning Jensen[1], Terje Thorsnes[1], Lilja Rún Bjarnadóttir[1], Jochen Knies[1,3]

[1]Geological Survey of Norway, P.O. Box 6315, Torgarden, 7491 Trondheim, Norway

[2] Department of Earth Sciences, Geological Institute, ETH Zürich, Sonneggstrasse 5, 8092 Zürich, Switzerland

[3] iC3: Centre for ice, Cryosphere, Carbon and Climate, Department of Geosciences, UiT The Arctic University of Norway, 9037 Tromsø, Norway

Contents of this file

Introduction

The supporting information includes translation tables that detail the relation between original and predicted substrate classes (Table S1) and depositional environments (Table S2). All spatial models used the same stack of predictor variables (Table S3), but additional predictor variables were also created. These included seabed substrate classes (Figure S1), sedimentary environment (Figure S2) and mud content (Figure S3). Spatial predictions of dry bulk density (Figure S4), organic carbon content (Figure S5) and sediment accumulation rates (Figure S6) were then used to calculate organic carbon stocks and accumulation rates (main document).

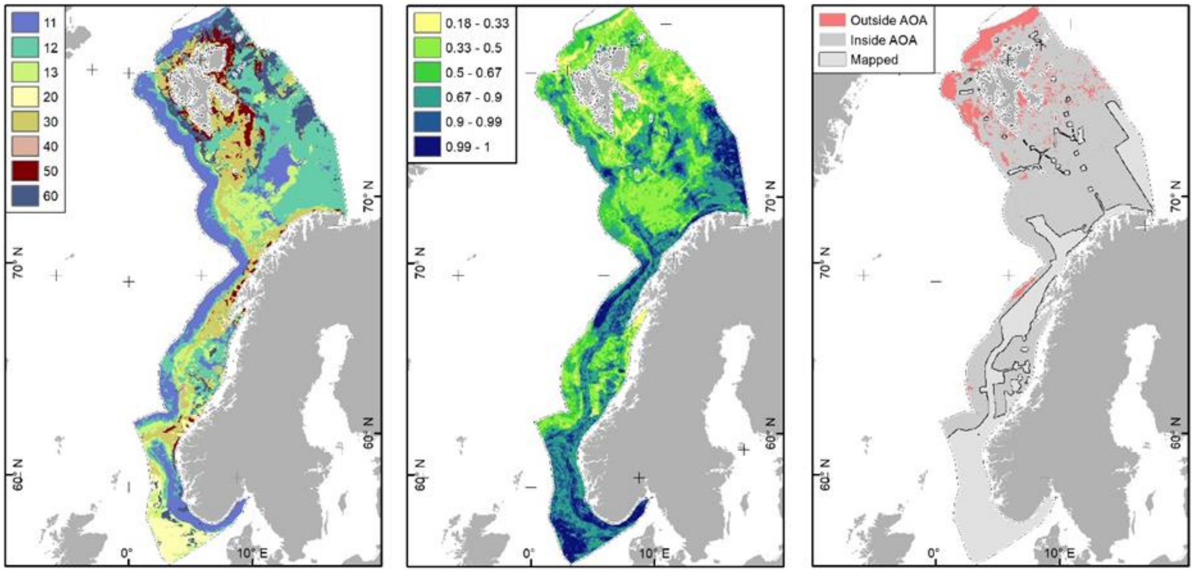

Figure S1. Seabed substrate classes on the Norwegian continental margin. Left - Predicted class: 11 – Mud, 12 – Sandy mud, 13 – Muddy sand, 20 – Sand, 30 – Coarse sediment, 40 – Mixed sediment, 50 – Rock and boulders, 60 – Mosaic seafloors. Centre – Confidence in the predictions on a scale between 0 (low) and 1 (high). Right – Area of applicability (AOA) of the model. Also shown are areas that were mapped by expert interpretation as part of the Mareano programme (Mapped).

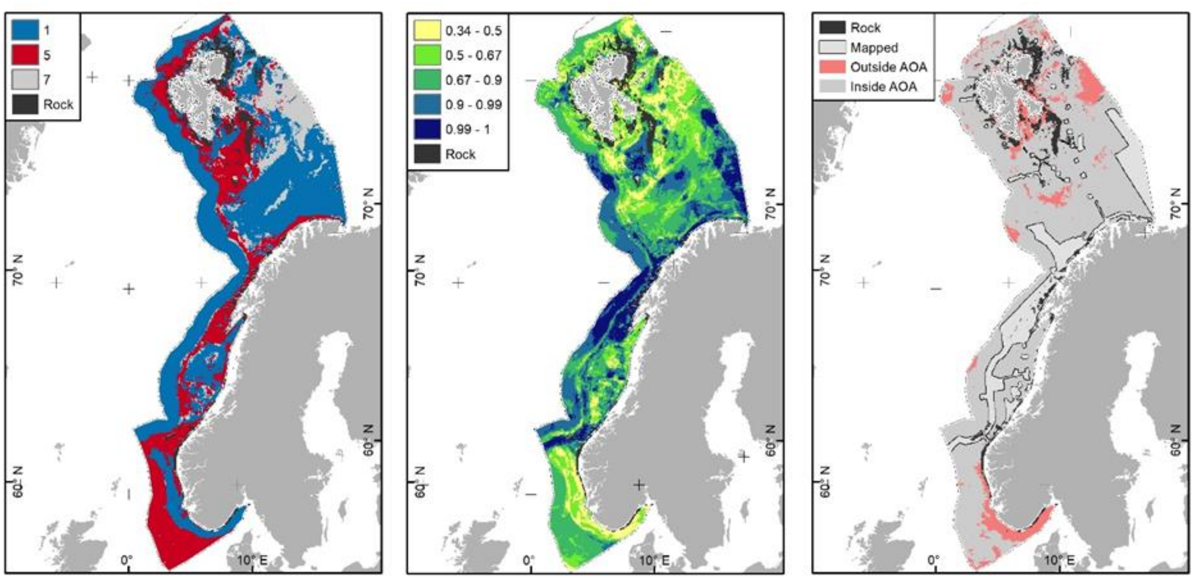

Figure S2. Sedimentary environment on the Norwegian continental margin. Left - Predicted environment: 1 – Deposition from suspension, 5 – Erosion or transport, 7 – No or very slow deposition. Centre – Confidence in the predictions on a scale between 0 (low) and 1 (high). Right – Area of applicability (AOA) of the model. Also shown are areas that were mapped by expert interpretation as part of the Mareano programme (Mapped). Areas predicted as rock in the substrate type model (Figure S1) were excluded from the analysis.

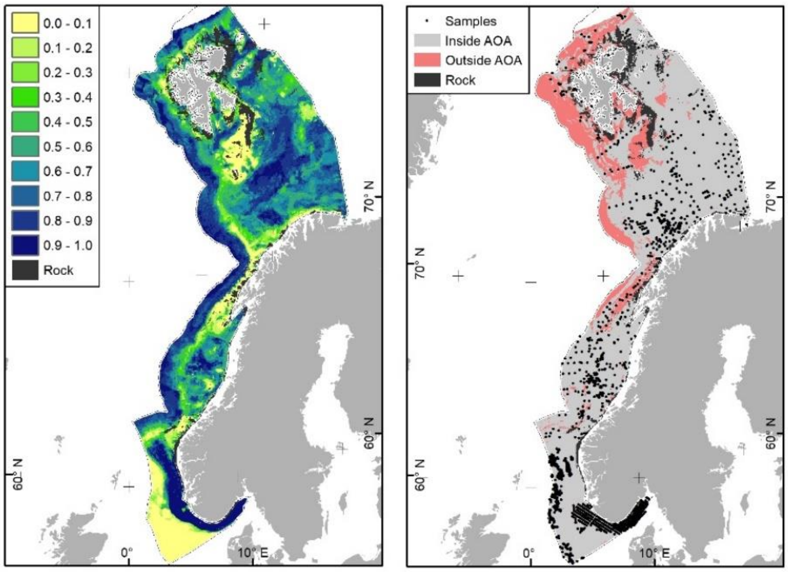

Figure S3. Mud (silt and clay) content of surficial sediments on the Norwegian continental margin. Predicted mud content expressed as fraction ranging between 0 and 1. Areas predicted as rock in the substrate type model (Figure S1) were excluded from the analysis. Note that mud content was only used as a predictor variable and predicted with random forest. Therefore, no estimates of prediction uncertainty were made.

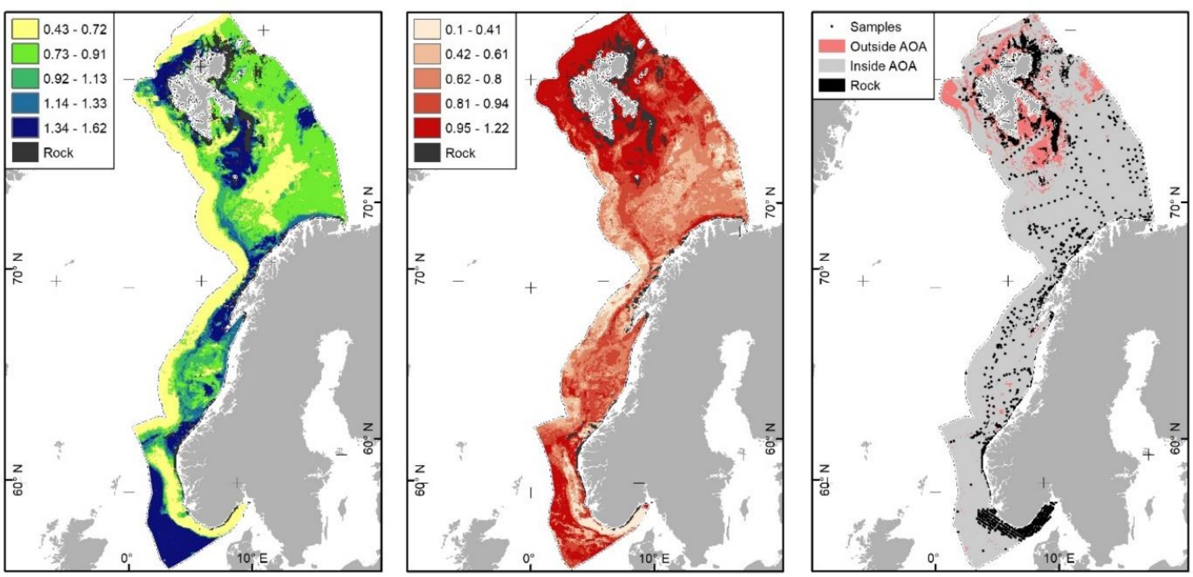

Figure S4. Dry bulk density of the upper 10 cm of surficial sediments on the Norwegian continental margin. Left – Predicted median value (g cm^{-3}). Centre – Prediction uncertainty (g cm^{-3}), expressed as the 90% prediction interval. Right – Area of applicability (AOA) of the model. Areas predicted as rock in the substrate type model (Figure S1) were excluded from the analysis.

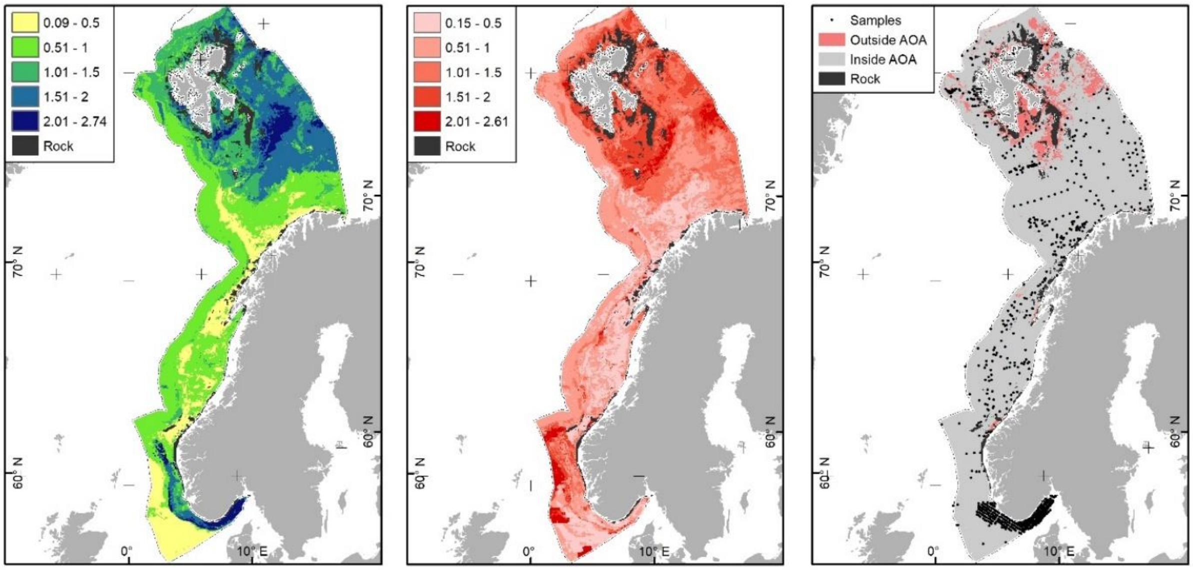

Figure S5. Organic carbon content of the upper 10 cm of surficial sediments on the Norwegian continental margin. Left – Predicted median value (weight-%). Centre – Prediction uncertainty (weight-%), expressed as the 90% prediction interval. Right – Area of applicability (AOA) of the model. Areas predicted as rock in the substrate type model (Figure S1) were excluded from the analysis.

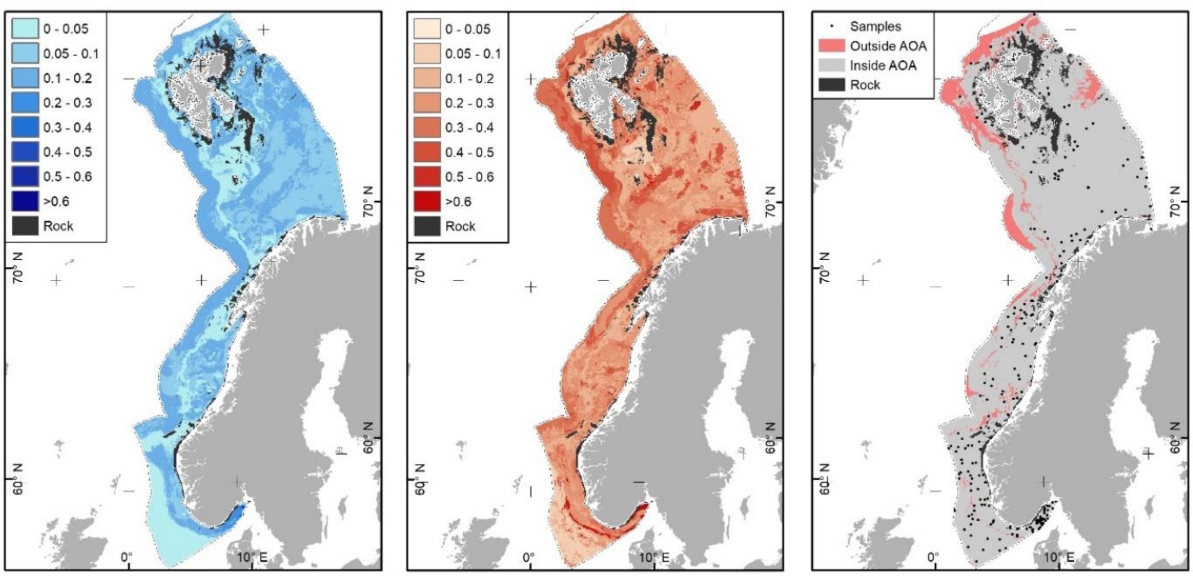

Figure S6. Sediment accumulation rates based on ^{210}Pb on the Norwegian continental margin. Left – Predicted median value (cm yr^{-1}). Centre – Prediction uncertainty (cm yr^{-1}), expressed as the 90% prediction interval. Right – Area of applicability (AOA) of the model. Areas predicted as rock in the substrate type model (Figure S1) were excluded from the analysis.

Table S1. Table detailing how the original substrate classes were translated into a simplified classification.

Original class	Simplified class (code)
Clay	Mud (11)
Mud	Mud (11)
Mud with sediment blocks	Mud (11)
Sandy clay	Sandy mud (12)
Sandy mud	Sandy mud (12)
Silt	Mud (11)
Muddy sand	Muddy sand (13)
Silty sand	Muddy sand (13)
Sand	Sand (20)
Gravelly mud	Mud (11)
Gravelly sandy mud	Sandy mud (12)
Gravelly muddy sand	Muddy sand (13)
Gravelly sand	Coarse sediment (30)
Muddy gravel	Mixed sediment (40)
Muddy sandy gravel	Mixed sediment (40)
Sandy gravel	Coarse sediment (30)
Gravel	Coarse sediment (30)
Gravel and cobbles	Coarse sediment (30)
Gravel, cobbles, and boulders	Rock and boulders (50)
Sand, gravel, and cobbles	Coarse sediment (30)
Mud/sand with cobbles/boulders	Mosaic seafloor (60)
Mud and sand with gravel, cobbles, and boulders	Mosaic seafloor (60)
Sand, gravel, cobbles, and boulders	Coarse sediment (30)
Compacted sediments or sedimentary bedrock	Rock and boulders (50)
Thin or discontinuous sediment cover on bedrock	Rock and boulders (50)

Table S2. Table detailing how the original sedimentary environment classes were translated into a simplified classification.

Original class	Simplified class (code)
Deposition from suspension	Deposition from suspension (1)
Deposition from suspension, local erosion of fine-grained sediments	Deposition from suspension (1)
No or very slow deposition	No or very slow deposition (7)
Deposition from bottom currents	Erosion or transport (5)
Erosion, local deposition of sediments in topographic lows	Erosion or transport (5)
Erosion	Erosion or transport (5)

Table S3. Summary of predictor variables used for spatial prediction.

Variable	Unit	Statistics	Time period	Source
Bathymetry	m	-	-	(GEBCO Bathymetric Compilation Group, 2019)
Topographic position index	m	Focal window sizes 25, 75, 125	-	Calculated from bathymetry
Distance to coastline	m	-	-	Calculated
Primary productivity	mg m^{-2} d^{-1}	Mean, maximum	2010 – 2019	Copernicus-GlobColour (https://doi.org/10.48670/moi-00281)
Chlorophyll-a concentration	mg m^{-3}	Mean, maximum	2010 – 2019	Copernicus-GlobColour (https://doi.org/10.48670/moi-00281)
Suspended particulate matter	g m^{-3}	Mean, maximum	2010 – 2019	Copernicus-GlobColour (https://doi.org/10.48670/moi-00281)
Surface partial pressure of CO_2	Pa	Minimum, mean, maximum, range	2010 - 2019	PISCES GLOBAL_REANALYSIS_BIO_001_029 (http://dx.doi.org/10.25607/OBP-490)
Sea ice concentration	-	Minimum, mean, maximum, range	2010 - 2019	GLORYS12V1 (https://doi.org/10.48670/moi-00021)
Dissolved molecular oxygen	mol m^{-3}	Minimum, mean, maximum, range	2000 - 2014	Bio-ORACLE v2.2 (https://www.bio-oracle.org/index.php)
Surface swept area ratio	-	Minimum, mean, maximum, range	2009 -2016	OSPAR (https://odims.ospar.org/en/search/?dataset=bottom_f_intensur)
Bottom current speed	m s^{-1}	Mean, maximum	2005 -2007	Nordic4k (http://hdl.handle.net/11250/113861)
Bottom temperature	°C	Minimum, mean, maximum, range	2005 -2007	Nordic4k (http://hdl.handle.net/11250/113861)
Bottom salinity	PSU	Minimum, mean, maximum, range	2005 -2007	Nordic4k (http://hdl.handle.net/11250/113861)